Electron tunnelling in electrochemical processes and in situ scanning tunnel microscopy of structurally organized systems

ARTICLE *in* ELECTROCHIMICA ACTA · JANUARY 1997

Impact Factor: 4.5 · DOI: 10.1016/S0013-4686(96)00333-7

Pergamon

PII: S0013-4656(96)00333-7

Electrochimica Acta, Vol. 42, No. 5, pp. 819–831, 1997

0013-4686/97 $17.00 + 0.00

Electron tunnelling in electrochemical processes and *in situ* scanning tunnel microscopy of structurally organized systems

Jens E. T. Andersen,[1] Alexei A. Kornyshev,[2] Aleksandr M. Kuznetsov,[3] Lars L. Madsen,[4] Per Møller[4] and Jens Ulstrup[1]**

[1]Chemistry Department A, Building 207, Technical University of Denmark, DK-2800 Lyngby, Denmark
[2]Institut für Energieverfahrenstechnik, Forschungszentrum Jülich, D-52425 Jülich, Germany
[3]The A. N. Frumkin Institute of Electrochemistry of the Russian Academy of Sciences, Leninskij Prospect 31, Moscow 117071, Russia
[4]Center for Advanced Electroplating, Building 425, Technical University of Denmark, DK-2800 Lyngby, Denmark

(Received 31 July 1996)

Abstract—The electronic tunnel factor in homogeneous long-range electron transfer (ET) systems has been characterized experimentally and theoretically in great detail. Outstanding questions, however, remain, for example interference in multiple ET routes and environmentally induced barrier fluctuations. Well characterized electrochemical long-range ET systems have also become available where the tunnel factor can be accurately deconvoluted from the total current. Intriguing new effects here are associated with the electrode charge or overpotential effects on the tunnel factor and with the feasibility of observation of critical current behaviour near phase transitions in thin films across which electron tunnelling occurs.

In situ scanning tunnel microscopy (STM) offers a conceptual and technical new frame for mapping of molecular ET routes through large adsorbate molecules with low-lying local fluctuating levels. Such a configuration would be representative of large transition metal complexes or redox metalloproteins. High-resolution images and new theoretical approaches to STM mapping of large adsorbates are, moreover reported. The independent *in situ* electrode potential control provides new, non-monotonous features in the current–voltage relations which differ from electrochemical ET behaviour at a single interface. Copyright © 1996 Elsevier Science Ltd

Key words: *In situ* STM, adsorbates, three-level processes, cytochrome *c*, azurin.

1. INTRODUCTION

Electron tunnelling in chemical and biological *homogeneous* electron transfer (ET) systems has been mapped in considerable detail [1–19]. This achievement is based on a combination of elaborate synthetic work, isolation and structural characterization of many redox proteins, their real or putative ET networks, and the feasibility of chemical and microbiological modification. At the same time this has warranted new theoretical work addressing tunnel features of the donor, acceptor, and intermediate molecular, protein, or solvent matter. Such features are, for example [1–4, 20–26]:

The distance and orientation of the donor, acceptor, and intermediate molecular groups;
the chemical nature of the intermediate material;
the supramolecular organization of organized multi-ET patterns of large protein complexes,
such as the photosynthetic reaction centres;
consistent treatment of electronic-vibrational interaction and fluctuating tunnel barriers in
long-range Condon and non-Condon ET modes;
extension to other processes such as multi-photon optical processes, long-range coupling of
electron spins *etc.*;

**Author to whom correspondence should be addressed.

extension to high-order through-space and through-bond routes, and to interference
between different routes;
vibrational coherence effects;
ET and critical phenomena in organized two- and three-dimensional systems.

Electrochemical ET has not witnessed a parallel evolution. Reasons for this have been: (a) the inadequate structural characterization of electrochemical thin film systems where tunnelling would be particularly important; (b) elusive structural deformation of large molecules at electrochemical interfaces, and (c) inadequate construction of metal and reactant electronic wave functions in the heterogeneous, electric field exposed interfacial region.

Prospects for preciser characterization of the electrochemical interface in relation to tunnelling are becoming available. These are rooted in the availability of new, stable mono- and multilayer electrochemical films, self-assembled into well characterized two-dimensional surface arrays [27–34]. Electrochemical data for tunnelling through the films are accurate enough that pre-exponential factors can be deconvoluted. Secondly, interfacial solid-electrolyte tunnelling is the fundamental origin of *in situ* scanning tunnel microscopy (STM), now in focus in interfacial structure and reactivity investigations. In contrast to other surface spectroscopy and diffraction techniques, STM images the interfacial structure to atomic or molecular resolution and therefore provides a basis for direct association of the tunnel parameters with molecular properties of the adsorbate or solvent between the substrate and tip.

We consider here some recent approaches to interfacial solid-electrolyte tunnelling. In Section 2 we briefly summarize, as a reference, some features of long-range homogeneous ET. In Section 3 we discuss new electrochemical ET theory based on density functional theory with special attention to potential-induced electron density lability. This effect has no immediate analogue in homogeneous ET. In Section 4 we address some new theoretical results and experimental data of importance to electrochemical ET coupled to critical phenomena in two-dimensional films. In Section 5 we extend these views to tunnelling through large adsorbates in resonance and off-resonance *in situ* STM modes.

2. ELECTRON TUNNELLING IN LONG-RANGE HOMOGENEOUS ET

The unimolecular rate constant for ET between a weakly interacting donor (D) and acceptor (A) molecular fragment, W_{DA}, is broadly represented by the equation [35–42]

$$W_{DA} = |T_{DA}|^2 \left(\frac{\pi}{\hbar^2 E_r k_B T}\right)^{1/2} \exp\left[-\frac{(E_r + \Delta G^0)^2}{4E_r k_B T}\right] \quad (1)$$

The activation Gibbs free energy incorporates the molecular and environmental reorganization Gibbs free energy, E_r and the driving force ΔG^0. The most important feature of the pre-factor is the electron exchange factor, T_{DA}, which incorporates the electronic wave functions of the donor, acceptor, and intermediate matter of all conceivable ET routes. k_B is Boltzmann's constant, T the temperature, and $2\pi\hbar$ Planck's constant. Figure 1 shows the common potential surface representation where the electronic energies are plotted against the nuclear coordinates. Ways of extending equation (1) to other system properties such as nuclear tunnelling, anharmonic coupling *etc.* are available [38–42]. We address here the tunnel factor T_{DA}.

The wave functions which constitute appropriate basis sets are the electronic Born–Oppenheimer wave functions of the donor, acceptor, and all intermediate bridge groups. In weakly interacting ET systems where tunnelling is explicitly important, the wave functions are commonly taken as a *diabatic* basis set, coupled in a perturbation scheme. This choice and the separation of the electronic Hamiltonians into zero order and perturbation terms are to a certain extent arbitrary. While present all the time in intramolecular ET systems the residual couplings which induce the transitions are, however, only important at the crossing of the Born–Oppenheimer potential surfaces. The major formal advantage of the diabatic representation is therefore that the time evolution (rate constant) is recast in terms of the separate donor, acceptor, and intermediate group electronic properties.

The way in which electronic wave functions, the distance and orientation variation of W_{DA}, specific ET routes, and the intermediate matter are reflected in T_{DA} can be illustrated by the following consideration. "Direct" through-space ET between D and A is always insignificant in *long-range* ET. The interaction is instead transmitted through the intermediate material represented by the molecular bridge groups $B1, B2, \ldots, BN$. Quantum mechanical

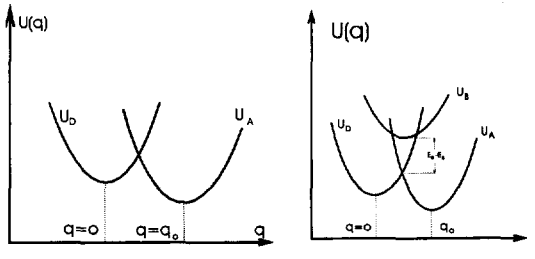

Fig. 1. Nuclear potential surfaces for two displaced electronic-vibrational states in homogeneous ET. Left: Direct ET between a donor and an acceptor state. Right: ET between a donor and an acceptor state *via* electronic coupling to a single intermediate, bridge group electronic-vibrational state.

perturbation expansion then brings T_{DA} to the form [41–46]

$$T_{DA} = V_{DA}^{(1)} + \sum_{j=1}^{N} \frac{V_{D(B1)}^{(1)} V_{(B1)(B2)}^{(1)} \cdots V_{(Bj)A}^{(1)}}{(E_D - E_{B1})(E_D - E_{B2}) \cdots (E_D - E_{Bj})}, \quad (2)$$

where the denominators are the energy gaps between the donor and bridge group LUMO's or HOMO's indicated by the subscripts while the $V^{(1)}$s are first order electron exchange factors coupling the molecular fragments indicated by the subscripts. Figure 1 also illustrates the ET configuration for a single bridge group. The energy gaps are thus the ones at the moment of ET, *ie* at the nuclear configuration where the reactants' and products' potential surfaces cross, and not equilibrium gap values. Equation (2) has the following further implications which extend to electrochemical and *in situ* STM tunnelling:

(1) Equation (2) applies when the energy gap is large and $V_{D(B1)}^{(1)} \ll E_D - E_{B1}$. When the intermediate state surface approaches the donor–acceptor state crossing, resonance and vibrational coherence arise, and equation (2) no longer applies in this simple form.

(2) Electron tunnelling, represented by $|T_{DA}|^2$ does not in general fall off exponentially with increasing donor–acceptor distance. Different routes, with positive or negative amplitudes may, moreover, contribute, and interfere constructively or destructively.

(3) The tunnel feature emerges conspicuously if all energy denominators can be assigned the same value Δ, and all bridge group couplings the same value β. The dominating term in equation (2) is then moreover the one of highest order ("N") where the whole space between D and A is filled. Equation (2) can then be reduced to the tunnel-like form [46]

$$T_{DA} \approx V_{DA}^{(N)} = \frac{\beta_D \beta_A}{\beta} \exp\left[-\frac{1}{a} \ln(\Delta/\beta) R \right], \quad (3)$$

where R is the donor–acceptor separation *along* the sequence of bridge groups, a the average bridge group extension, while β_D couples D with the first bridge group and β_A couples A with the Nth bridge group. Tunnelling thus decays faster the larger the gap and the weaker the coupling. In this sense protein is a better tunnel "conductor" than water which is again better than vacuum. The bridge groups, finally, couple the donor and acceptor levels *electronically* just as in tunnelling. The levels are only populated when $\Delta \to 0$ and resonance between the three levels is approached, whereas equations (2) and (3) apply only far from resonance.

The views represented by equations (1)–(3) have been substantiated by many data based on intramolecular ET in synthetic covalent donor–acceptor systems and in metalloproteins [1–5, 10, 12, 14].

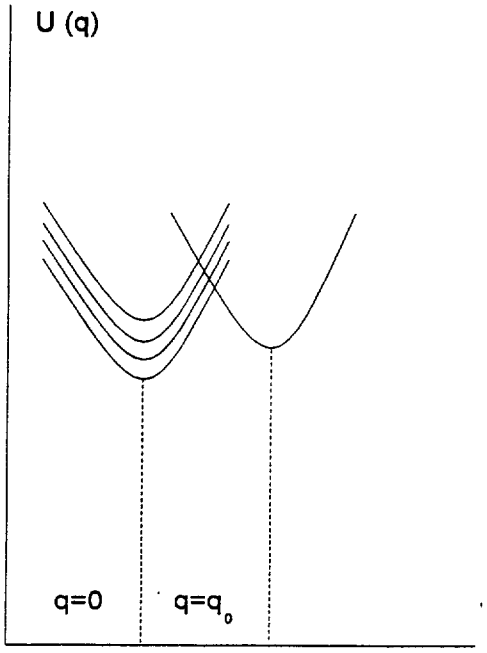

Fig. 2. Nuclear potential surfaces for two displaced electronic-vibrational states in electrochemical ET with a continuous manifold of in the initial potential well.

The simplicity of equations (1)–(3) should, however, urge towards care in specific application. Two kinds of reservation are appropriate:

(4) Many experimental long-range ET systems rest on photochemically induced processes and excited electronic states. These are not always far from intermediate group electron or hole states, and may correspond to small energy gaps. This would lead to intermediate state population and sequential or vibrationally coherent two-step processes.

(5) The tunnel factor is the one that prevails at the moment of ET. Nuclear reorganization to a configuration intermediate between the reactants' and products' equilibrium configurations must, however, occur prior to ET. T_{DA} in equation (1) can therefore not in general be simply separated from the nuclear factor but takes the more general form $T_{DA} \to T_{DA}(\Delta G^0; T)$ [24, 47]. Further entanglement arises from the break-down of the Condon approximation for separation of electronic and nuclear motion. The importance of these effects depends on specific system properties. For example, self-consistent calculation of the electronic-vibrational interaction for exponential wave functions in a homogeneous isotropic dielectric medium gives large effects for ET distances in the range 10–20 Å, *ie* the tunnel factor rises by several orders of magnitude due to the barrier fluctuations [48]. Inclusion of the reactant molecules in a solvent cavity would, understandably give much smaller environmentally induced fluctuation effects.

Equations (1)–(3) and the following discussion can serve as a reference for tunnelling in electrochemical

ET or *in situ* STM. The form of the tunnel factor, however, points to some of the difficulties expected. The electronic properties of weakly interacting *molecular* reactants may carry over to the interfacial ET modes but the electronic properties of the intermediate bridge groups in the electric field exposed interfacial region are much more elusive. The same applies to the wave functions of the metal which extend into the solution region. Depending on the importance assigned to repulsive solvent pseudopotentials or attractive polarization, wave function contraction into the metal or expansion into the solution can thus be expected. These opposite trends have, furthermore been forwarded to account for interfacial capacitance [48–51], and for work function effects and tunnel enhancement [52, 53], respectively. Such conflicting emphasis has been avoided in homogeneous ET where a much more detailed level of experimental and theoretical characterization has been achieved.

3. LONG-RANGE ELECTROCHEMICAL ET AND DENSITY FUNCTIONAL THEORY

3.1 Some classes of long-range electrochemical ET

Elastic, resonance, and inelastic electrochemical tunnel concepts in electrochemical ET were introduced in the 1970s and 1980s [54–63]. Systems were thin metal oxide and polymer films, semiconductor band gaps, cross-linked conducting polymers, mono- and multilayer electrocatalysts, and ET *via* metal adsorbate states. Long-range electrochemical ET more recently includes charge transport *via* localized redox centres in thin surface films [61, 64]. Electron hopping is thus competitive with diffusion of the film-enclosed molecular redox entities when electron exchange is fast, but charge transport patterns are frequently entangled by other features such as counter ion and migration, film inhomogeneity *etc.*

Metalloproteins constitute another system class associated with long-range electrochemical ET [65–67]. The surface organization of the molecules is largely unknown, although *ex situ* and *in situ* scanning probe microscopy (*cf.* below) points to organized array formation [68–73]. Crystal structures also show that the redox centres can be located "inside" the protein. Long-range effects are supported by the dramatic activation induced by molecular "wiring" [74] and the common need for promoters [65–67]. Directional tunnelling is thus in principle feasible also in electrochemical metalloprotein ET but lack of adsorbate structural information has kept mechanistic detail to a low level compared with homogeneous ET.

Photochemically induced tunnelling has been reported [75–77]. Small barriers and decay factors are here conceivable. Detailed tunnel characterization has been achieved recently from current–voltage relations of electrochemical ET through variable-length alkyl thiols self-assembled on gold electrodes [29–34]. Several kinds of molecular reactants have been used, in particular $[Ru(NH_3)_6]^{2+/3+}$ (freely mobile), ferrocene/ferrocinium (covalently linked), and cytochrome *c* (adsorbed). The structural order of such films is reflected in the vibrational spectra, X-ray diffraction, and other properties. Collective dynamics, including phase transitions are also characterized in considerable detail. Properties of importance to the tunnel features include [33, 34]: (a) Disentanglement of the nuclear factor from the pre-factor; (b) small values and approximately exponential film thickness dependence of the pre-factors. This has been brought to cover many orders of magnitude in the current, corresponding to a distance variation from $\approx$8–27 Å, or a tunnel decay factor of 1.1–1.3 $Å^{-1}$. Some distance variation of the reorganization Gibbs free energy can be expected over such a wide range but these results remain as some of the most conspicuous reflections of electrochemical electronic tunnelling; (c) a characteristic overpotential variation of the tunnel factor [29]. Such a variation is expected, *cf.* below, although the *observed* variation was in fact opposite to the effect expected. Overall reports such as those in [29–34] point to the feasibility of constructing well characterized long-range electrochemical ET systems which reflect details of electron tunnel phenomena.

3.2 Diabatic electrochemical current–voltage relations

The cathodic current density at the overvoltage η is, for a weakly interacting molecule [41, 78–80]

$$j_c = eC_{ox}\delta z\int d\epsilon \rho(\epsilon) f(\epsilon)\, W_c(\epsilon;\eta), \qquad (4)$$

where e is the electronic charge, $\rho(\epsilon)$ the density of states, $f(\epsilon) = [1 + \exp(\epsilon - \epsilon_F)/k_BT]$ the Fermi function, ϵ_F the Fermi energy, δz the (small) z-range perpendicular to the electrode surface contributing to the tunnel factor, and W_c the rate constant (s^{-1}) for ET from a given level ϵ. W_c can be given a form analogous to equation (1)

$$W_c(\epsilon;\eta) = |T_{DA}(\epsilon;\eta;z_0)|^2 A \exp[-F_c^{\neq}(\epsilon;\eta)/k_BT,$$

$$A = (\pi/\hbar^2 E_r k_B T)^{1/2};$$

$$F_c^{\neq}(\epsilon;\eta) = [E_r + e\eta - (\epsilon - \epsilon_F)]^2/4E_r, \qquad (5)$$

where z_0 is the distance of the molecular centre from the surface. An analogous form applies to anodic currents. Double layer corrections (work terms), field penetration *etc.* can be added as warranted.

Equations (4) and (5) have the form of a weighted sum of independent contributions from all the metallic levels (Fig. 2). Validity conditions for this view are available [79, 80]. Presently we note that energies close to the Fermi energy dominate over

broad overpotential ranges $|e\eta| < E_r$, converting equations (4) and (5) to the approximate form

$$j_c \approx j_{co} \exp[(e\eta)/2k_BT - (e\eta)^2/4E_rk_BT],$$

$$j_{co} = eC_{Ox}\delta z\rho(\epsilon_F)f(\epsilon_F)\delta\epsilon$$

$$|T_{DA}(\epsilon_F; \eta = i0; z_0)|^2 A \exp[-E_r/4k_BT], \quad (6)$$

where j_{co} is the exchange current and $\rho(\epsilon_F)\delta\epsilon \approx k_B\rho(\epsilon_F)$ the number of levels effectively contributing. All overpotential dependence is thus assigned to the activation Gibbs free energy $F_c^{\neq}(\epsilon_F; \eta)$. The quadratic overpotential dependence of the latter is modified if vibrational frequency changes, anharmonicity *etc.* is important. Other modifications can be expected from *long-range* ET for which $|T_{DA}(\epsilon; \eta; z_0)|^2$ may vary comparably to $F_c^{\neq}(\epsilon; \eta)$ with the overpotential [81].

3.3 Electron density lability in long-range electrochemical ET

With a view on new long-range electrochemical ET the electron exchange factor in equations (5) and (7), $T_{DA}(\epsilon; \eta; z_0)$ warrants attention. By Wolfsberg–Helmholz-like approximations $T_{DA}(\epsilon; \eta; z_0)$ is approximately related to the overlap integral between the molecular $\Psi(\tilde{r}; z_0)$ and metallic wave functions $\psi_\epsilon(z; \tilde{R}; \epsilon)$

$$|T_{DA}(\epsilon; \eta; z_0)|^2 \approx [V_{DA}(z_0)]^2 \int dz\, d\tilde{R}\psi(\tilde{r}; z_0)\psi_\epsilon^*(z; \tilde{R}; \epsilon), \quad (7)$$

where $\tilde{r} = (z, \tilde{R})$, $\tilde{R}$ being the lateral radius vector, and $V_{DA}(z_0)$ the molecule–electrode interaction. The wave functions, and their potential dependence and interaction with the environment are thus needed. As noted, this is feasible to various degrees of detail for the molecular part but has not been achieved self-consistently for the metallic wave functions.

Approaches to the interfacial electronic structure resting on the *overall* electronic density rather than the *individual* wave functions, however, offer clues to new electronic effects imposed by the field and environment [81–84]. By the Kohn–Sham scheme [85] the density functional effects can also be self-consistently related to the wave functions. The metal and molecular electron density are, respectively,

$$n(z; \epsilon; \eta) = \rho(\epsilon)f(\epsilon)|\psi_\epsilon(z; \epsilon; \eta)|^2;$$

$$\Omega(z; z_0 = \int d\tilde{R}|\Psi(z; \tilde{r}; z_0)|^2. \quad (8)$$

A key observation is now that the quantities in the overlap integral and density functionals assume significant values in different regions of space and energy, so that their products are dominated by narrow ranges of ϵ and z [81]. For example, $f(\epsilon)$ drops rapidly when $\epsilon > \epsilon_F$ whereas $|\Psi(z; \epsilon; \eta)|^2$ outside the metal rises with increasing ϵ. As a result $n(z; \epsilon; \eta)$ has a pronounced maximum close to ϵ_F. Even though the current density cannot in general be recast in terms of electron densities, this representation is still a good approximation over broad energy ranges. By such reasoning the current density takes the approximate form [81]

$$j_c \approx eC_{ox}\delta z[V_{DA}(z_0)]^2(\delta\epsilon/\Delta\epsilon)\, M(\eta)\exp[-F_c^{\neq}(\epsilon_{cat}^*/k_BT] \quad (9)$$

where $\epsilon_{cat}^* \geqslant \epsilon_F$, $\delta\epsilon$ and $\Delta\epsilon$ are two narrow energy intervals ($\approx k_BT$) while $M(\eta)$ is the electronic density overlap function

$$M(\eta) = \int dz|\Omega(z; z_0|n(z; \epsilon_{cat}^*; \eta). \quad (10)$$

An analogous form where $M(\eta) \to 1 - M(\eta)$ applies to the anodic current density. Equations (9) and (10) thus imply that there is a new overpotential dependence in the electronic tunnel factor, important specifically in long-range ET.

Equations (8)–(10) can be combined with specific representations of the molecular wave function and the metallic density functional. Such analysis is provided in [81] for the broadly representative exponential form

$$|\Psi(z; \tilde{R}; z_0)|^2 = (\gamma^3/8\pi)\exp\{-\gamma[R^2 + (z - z_0)^2]^{1/2}\} \quad (11)$$

where γ is the distance decay factor (*cf.* equations (2) and (3)), and the jellium trial functional [82]

$$n(z; \eta) = n_+\{\{1 - \tfrac{1}{2}\exp[\beta(z - \bar{z})]\}\theta(\bar{z} - z) + \tfrac{1}{2}\exp[\beta(\bar{z} - z)]\theta(z - \bar{z})\}$$

$$\beta = \beta_0 + a\sigma + b\sigma^2 + d\sigma^3; \quad \bar{z} = \sigma/n_+ \quad (12)$$

where σ is the excess surface charge density, n_+ the bulk metallic electron density, $\theta(x)$ the step function while the decay function β is determined by σ and a set of expansion coefficients. Equations (11) and (12) combined with equation (10) give the density overlap function [81]

$$M(\eta) = A(\gamma; \beta; z_0; n_+)\exp[-\beta(z_0 - \bar{z})] + B(\gamma; \beta; z_0; n_+)\exp[-\gamma(z_0 - \bar{z})] \quad (13)$$

where the coefficients $A(\gamma; \beta; z_0; n_+)$ and $B(\gamma; \beta; z_0; n_+)$ are weakly varying functions.

Equations (8)–(13) represent the electron density or tunnel lability induced by the overpotential variation. By available procedures dielectric and other environmental effects can also be incorporated. The density functionals along with their overpotential dependence and environmentally induced fluctuations can finally be converted to the corresponding wave functions. The following observations have been noted [81]:

(A) Equations (12) and (13) show that the jellium profile is shifted out of the metallic region as the surface is charged negatively while it contracts into the metal when the surface is charged positively. At the same time the profile *shape* is changed as β also depends on the charge density. This would lead to more facile tunnelling at given voltages on the negative than on the positive side of the potential of

zero charge. This expectation is substantiated by numerical calculations for representative values of the electron density, n_+, the position of the discharging molecule z_0 (2.5–11 Å), and the molecular decay factor γ(1–2 Å^{-1}).

(B) The electronic lability effect is unimportant for small distances and high-density metals such as Au and Hg. The effect can, however, be notable for low- and intermediate-density metals such as Ag, and tunnel distances in excess of ≈ 10 Å.

(C) As an illustration, the jellium-based tunnel factor for Ag and an ET distance of 11 Å varies by up to three orders of magnitude in the voltage range ≈ 0.3 V due to the charge density lability. In comparison, the nuclear factor varies between three and five orders of magnitude depending on the value of the reorganization Gibbs free energy.

Fast electrochemical techniques including combination with laser temperature jump techniques have reached a level where the pre-exponential tunnel factor can be deconvoluted accurately from the total current [34]. Electrochemical ET across variable-length self-assembled thiol monolayers to which ferrocene or other redox centres have been covalently tethered, constitute suitable probe systems in this respect. Overpotential effects of the kind described do not, however, emerge from these particular systems which otherwise unambiguously disclose tunnel features. This could be because the electrode is a high-density metal, or the interfacial capacitance is small, giving a small charge density variation over the accessible potential range. Investigations analogous to those in [29–34] using silver or lower-density metal and semi-metal electrodes might come closer to display the electronic density lability effects.

4. CONTINUOUS PHASE TRANSITIONS IN INTERFACIAL TUNNEL SYSTEMS

A new perspective is associated with phase transitions in thin films across which electrons tunnel. First order transitions in organic monolayer systems and their reflection in electrochemical ET have been reviewed [86]. The reflection is mostly in the form of abrupt changes in tunnel or activation Gibbs free energy parameters. These can be incorporated phenomenologically in electrochemical ET theory. More composite behaviour can be expected if the phase transition is combined with the adsorption isotherm of the organic monolayers.

The effect of *continuous* phase transitions and critical behaviour of the order parameters on the electrochemical ET rate have been addressed more recently [26, 87]. Critical ET behaviour near continuous two-dimensional phase transitions is of notable interest and holds intriguing perspectives in relation to other two-dimensional systems among which lipid bilayers stand out conspicuously [88]. Further interest would relate to transitions in layers of magnetic electrocatalysts such as transition metal complexes based on phthalocyanins or porphyrins. Such transitions might be strikingly reflected in electrochemical processes of paramagnetic depolariser molecules such as dioxygen. The transitions finally hold perspectives in relation to protein and other macromolecular organization on solid surfaces.

The central conceptual frame of continuous phase transitions in relation to electrochemical ET is coupling of the current to the local value of a suitable vectorial or scalar order parameter $s(\vec{r})$ such as the density in the two phases [26, 87]. The *local* current is thus

$$j = j_0 \exp\left[b|s(\vec{r})|\right] \tag{14}$$

where $\vec{r}$ is the three-dimensional space coordinate. This form implies that the order parameter controls either the tunnel factor or the activation Gibbs free energy irrespective of its sign. b thus takes the schematic but representative form

$$b = \Gamma - \delta E_A/t, \tag{15}$$

where Γ represents the increments in the tunnel factor, δE_A in the activation Gibbs free energy, and $t = T/T_c$ where T_c is the critical temperature. The *mean* current is

$$j = j_0 Z^{-1} \int \mathscr{D}\left[s(\vec{r})\right] \exp\left[b|s(\vec{r})|\right] \exp\left\{-F[s(\vec{r})]/k_B T\right\},$$
$$Z = \int \mathscr{D}\left[s(\vec{r})\right] \exp\left\{-F[s(\vec{r})]/k_B T\right\}, \tag{16}$$

where $\mathscr{D}[s(\vec{r})]$ denotes functional integration with respect to $s(\vec{r})$.

Equation (16) frames in general terms the average current coupled to an order parameter. It is important that coupling is to the *local* value of $s(\vec{r})$ rather than its average because critical slowing down close to the transition would inevitably cause the fluctuations to be slower than the ET process itself. Equations (14)–(16) must be coupled with suitable Hamiltonians for the collective order parameters. The Landau–Ginsburg mean field functional [89]

$$F[s(\vec{r})] = F_0 + \tfrac{1}{2}\int d\vec{r}\,d\vec{r}'\,\Phi(\vec{r} - \vec{r}')s(\vec{r})s\vec{r}') + \tfrac{1}{2}C\int d\vec{r}[s(\vec{r})]^4 \tag{17}$$

is both a suitable starting frame for fluctuations and criticality in long-range ET and appropriate in relation to the degree of detail presently available experimentally. The susceptibility function in the quadratic term holds a local and a non-local part

$$\Phi(\vec{r} - \vec{r}') = A(T)\delta(\vec{r} - \vec{r}') + X(\vec{r} - \vec{r}') \tag{18}$$

where the critical behaviour is reflected in the quantity $A(T)$, *ie* $A(T) > 0$ when $T > T_c$ and < 0 when $T < T_c$.

Equations (14)–(18) were analyzed extensively in the recent reports to which we refer for formal details and discussion of experimentally investigated systems [26, 87]. We note that the resulting current–temperature relations are analytical and reduce to simple forms at the transition temperature where an extremum emerges. The extremum is, further either a

sharp maximum (peak) or a minimum (dip) depending on the sign of the coupling parameter b. The latter observation reflects that tunnelling or nuclear activation can be favoured or disfavoured, respectively, as the system crosses over from the ordered to the disordered state.

Critical dynamic behaviour is broadly known for two-dimensional magnetic systems. First order phase transitions in electrochemical overlayers have also been broadly characterized but real or putative continuous phase transitions in critical electrochemical *current* behaviour are rare. Two recent examples are discussed in [87]. One of these, *viz.* $[Fe(CN)_6]^{3-}$ reduction at $C_{18}H_{37}S$-covered gold electrodes [90] is illustrated in Fig. 3. The current first rises gradually with increasing temperature (at given overvoltage). At 328 K within a few degrees the rise continues abruptly, followed by a similar rapid drop from the peak value. This system thus exhibits important features resembling critical ET behaviour, and corresponding to more facile ET in the ordered low-T state. This would be in line with better organized through-bond ET routes or partial nuclear freezing in the ordered state compared with the disordered state. Distinction is not presently feasible but likely to be attainable, by approaches such as those discussed in the previous Section. This kind of system might therefore hold interesting clues to mechanisms of electrocatalysis and biological membrane or protein processes.

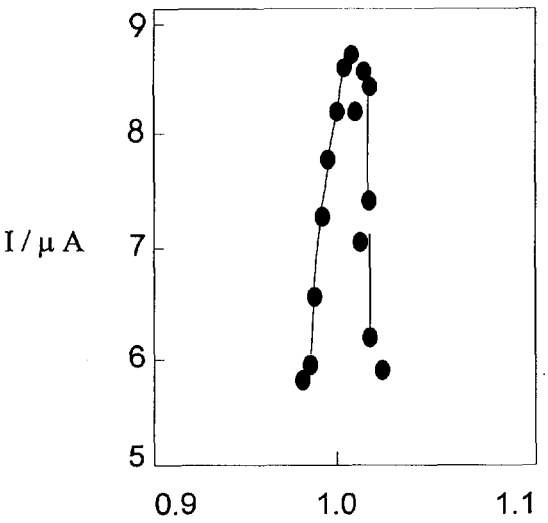

Fig. 3. Dependence of the electrochemical current for $[Fe(CN)_6]^{3-}$ reduction at $C_{18}H_{37}S$-covered gold electrodes on T/T_c where T_c (= 328 K) is the critical temperature for phase transition in the film. T-corrected overpotential −250 mV. Data from [90].

5. INTERFACIAL ET AND *IN SITU* STM OF LARGE ADSORBATE MOLECULES

5.1 STM of molecular adsorbates with multiphonon electronic-vibrational interaction

STM in the *in situ* mode has opened exciting perspectives for direct imaging of the structure and dynamics of the electrode–electrolyte interface and for two-dimensional adsorbate organization [68–72, 91, 92]. At the same time the physical mechanism of the imaging process holds puzzles. For example, the contrast relative to the background can be shifted in certain potential ranges, and the apparent tunnel distance sometimes appears unphysically large. From electron micrographs the surfaces of seemingly very good tips further, appear virtually flat on the μm scale. Other puzzling issues are associated with tip-induced disturbances in the gap region, and with very high current density flow through the adsorbates.

Theoretical approaches to *in situ* STM have focused on different features, in particular:

(A) Continuous dielectric solvent representations combined with jellium representations of the substrate and tip. Focus has been on the electronic solvent polarization which stimulates tunnelling relative to vacuum (*cf.* above) [52, 53].

(B) Addition of local pseudopotentials to a continuous background [52, 53]. Depending on their attractive or repulsive nature, tunnelling would then be stimulated or hampered, respectively, similar to observations from jellium protrusion in single-interfacial electrochemical systems [48–50].

(C) Approaches based on networks of "quantum dots", *ie* local gap levels broadened by interaction with other "dots" or with the electrodes [93]. As for pseudopotential-based tunnel conductivities the "dots" represent molecular properties, and interference including "resonances", "dips", and other features in the conductance–voltage relations emerges from suitable "multi-dot" organization.

(D) Time correlation of the tunnel process with atomic adsorbate diffusion or molecular adsorbate reorientation. This provides a frame for noise patterns [94, 95]. The full expression for the current–current time correlation function $K(t) = \langle j(t)j(0)\rangle - \langle j^2\rangle$ scales differently for isotropic and strongly anisotropic diffusion [94, 95]. $K(t)^{-1} - K(0)^{-1} \sim t$ for the isotropic case, with the coefficient proportional to the diffusion coefficient, while $K(t)^{-2} - K(0)^{-2} \sim t$ for strongly anisotropic diffusion, with the coefficient proportional to the diffusion coefficient along the axis of easy diffusion. This provides the typical noise frequency spectra which are, for example, proportional to ln ω at small frequencies. The ln ω law has recently been observed in *ex situ* measurements of oxygen diffusion on Si(111) [96] in accordance with the theory. The strongly anisotropic diffusion near frizzy steps [97] is also in line with the pattern expected from the theory.

(E) Resonance tunnelling coupled to a phonon system, combined with Breit–Wigner equations of motion [98]. Strong electronic-vibrational coupling

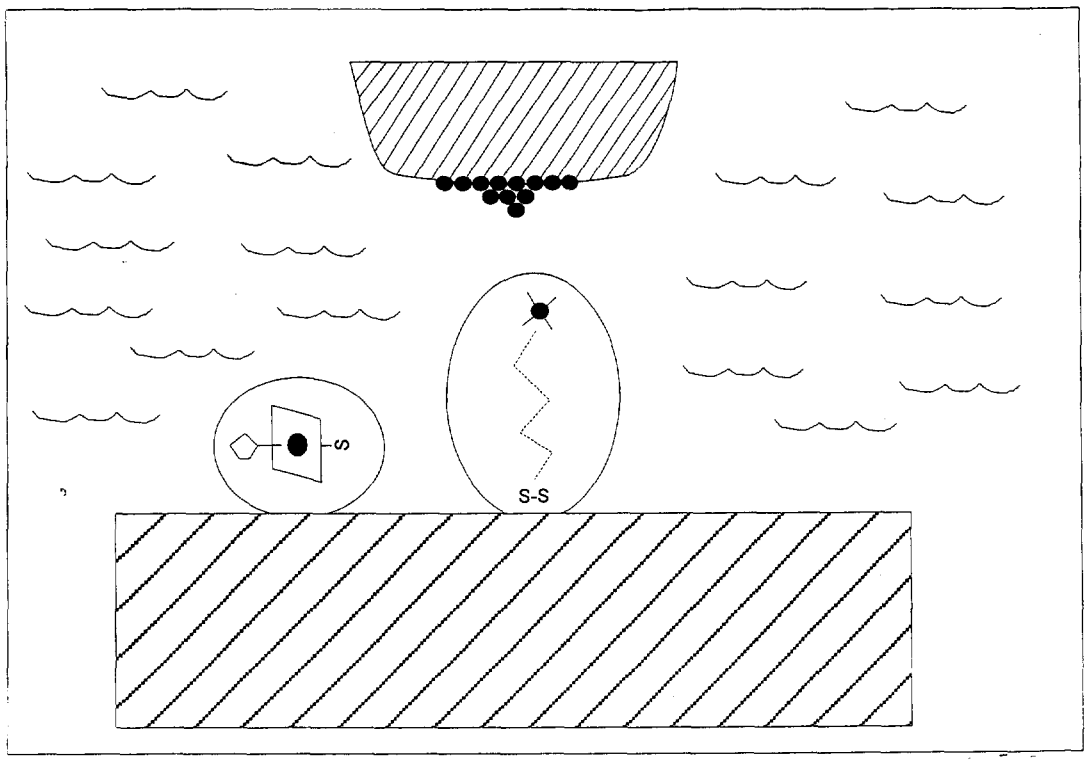

Fig. 4. Schematic *in situ* STM configuration of large adsorbate molecules. The two molecules shown are the redox metalloproteins cytochrome *c* [73] and azurin. The metal centre in the former is the heme group while it is a blue Cu-centre in the latter. S–S indicates the disulphide group of azurin.

gives considerable resonance congestion, in concordance with conductivity data for semiconductor systems.

(F) STM of a solvated molecular adsorbate level—representative of the central metal ion in a large transition metal complex or a redox metalloprotein—has finally been viewed as a three-level electronic process analogous to other three-level coherent or superexchange thermal and optical processes. This view, first introduced in [99], incorporates diabatic and adiabatic limits, resonance and off-resonance features, and vibrationally coherent tunnel processes [100, 101], and provides interesting relations to resonance Raman scattering. Some elements of this approach are discussed below.

(G) STM of a solvated molecule has, finally been viewed as a resonance process in which a discrete adsorbate level coupled to local or environmental nuclear modes is broadened by interaction with resonating substrate and tip levels [102, 103].

The approaches in [100–102] can be viewed in relation to reported *ex situ* and *in situ* STM imaging of metalloproteins such as nitrogenase [104], cytochromes *c* [73, 105], c_3 and c_{551} [106], and the multi-copper protein laccase [107]. The metal centres (iron and copper) are spatially separated from the solvent and the electrodes by protein. They also have local redox levels much lower in energy than the surrounding protein or solvent. The strong coupling of the local levels to the environment implies that the protein or solvent HOMO or LUMO levels constitute *fluctuating* barriers for the tunnel process. The local metallic level may in some cases remain high in energy and represent a fluctuating barrier indentation. A more representative situation could, however, be that the local level approaches the Fermi level of the substrate or tip closely enough to be temporarily *populated* in the STM process. The STM process then resembles electrochemical ET but exhibits important differences caused by the two-step nature of the process and the possible vibrational coherence in the intermediate populated state.

Figures 4–6 illustrate the STM patterns appropriate to this view [73, 100, 101]:

(1) The local level at the nuclear configuration $q = 0$ is initially well above the Fermi levels of both tip (ϵ_{LF}) and substrate (ϵ_{RF}). In contrast to electrochemical ET, tunnelling through an indented barrier is feasible in this configuration.

(2) Fluctuations, induced by the nuclear environment take the level to positions close to the Fermi level of the negatively biased electrode $q = q_1$. This requires activation but in return the barrier indentation is now much deeper, even to the extent of temporary population.

(3) Three-level STM in the populated intermediate state mode exhibits multifarious behaviour depending on the energy gaps, coupling strengths, and tunnel

barriers. The following three patterns in particular should be noted:

(3i) The electron may proceed "directly" from a given donor, say substrate level, to a *resonating* acceptor (tip) level *via* the local molecular level in resonance with both the delocalized substrate and tip levels. Any nuclear configuration between q_1 and q_4 contributes to this mechanism (say q_2 and q_3, Fig. 5). This is the mechanism considered in [102] and [103].

(3ii) Each of the substrate and tip levels is, however, separated only infinitesimally from a continuous manifold of other levels. Unless the coupling between the local level and the acceptor level (the positively biased electrode) is strong, and the adiabatic limit approached, continued nuclear fluctuations are therefore likely to take the intermediate level to a position *between* the Fermi levels of the two electrodes *before* the second ET step occurs (say from q_1 to q_2 in Figs 5 and 6). Nuclear dynamics on the intermediate potential surfaces is therefore important and the overall process composed of a manifold of vibrationally coherent two-step processes [100, 101].

(3iii) When the electronic coupling between the local level and each of the substrate and tip level sets is *weak*, and tunnel features strongly conspicuous (the strongly diabatic limit), then the second transition is unlikely to proceed before the populated intermediate level has relaxed to nuclear equilibrium below both Fermi levels. The second step is then induced only after renewed nuclear fluctuations in the intermediate state.

(4) Analogous considerations apply to hole transfer where a filled molecular level below the two Fermi levels is first excited to energies above these levels. This is followed by ET from the molecular adsorbate to the positively biased electrode, and subsequently by ET from the negatively biased electrode to the, now, empty molecular level.

The discussion above refers to systems with suitably spatially separated electronic centres but extends to stronger adsorbate–electrode interactions corresponding to adiabatic three-level STM processes. Presently, we conclude that distinction between the diabatic fully resonating three-level mode, and the populated, vibrationally partly or fully relaxed STM modes is convenient. This is the basis of the following discussion.

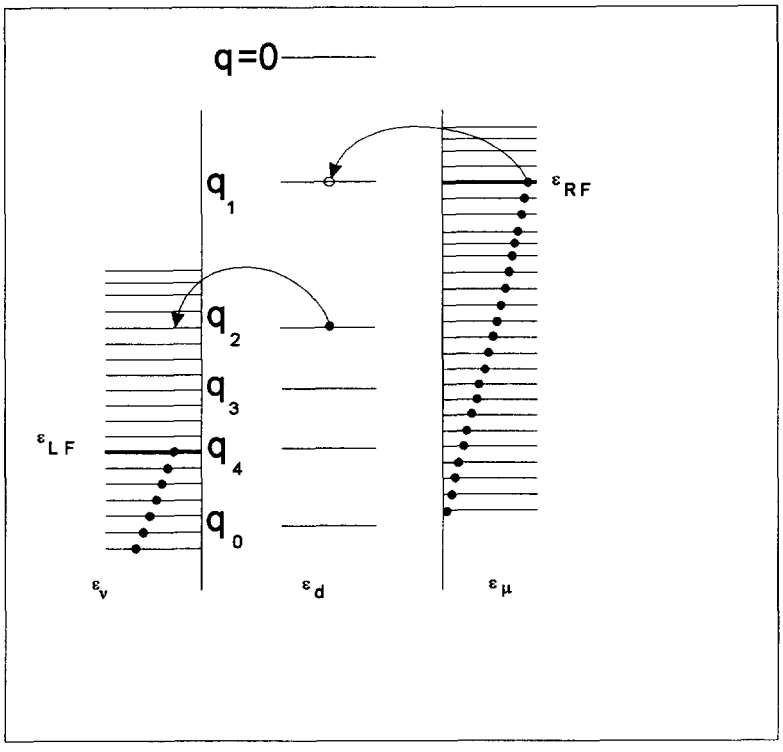

Fig. 5. Adsorbate level between two continuous metallic level distributions. Electron tunnelling is from the negatively (right) to the positively biased electrode (left). Tunnelling is feasible when fluctuations take the adsorbate level from the initial location well *above* both Fermi levels (ϵ_{RF} and ϵ_{LF}) to a location *between* the Fermi levels. All level pairs between ϵ_{RF} and ϵ_{LF}, *ie* ϵ_μ and ϵ_v can be involved. The configuration q_1 represents ET from the Fermi level of the negatively biased electrode. q_2 is an intermediate configuration from which the electron would be coherently transmitted to the positively biased electrode *above* the Fermi level. q_3 would be a similar level configuration. If, following the first ET step at the configuration q_4 the adsorbate has not succeeded to transmit the electron before reaching the Fermi level of the positively biased electrode (ϵ_{LF}), then the electron is trapped on the molecule and renewed thermal activation is needed.

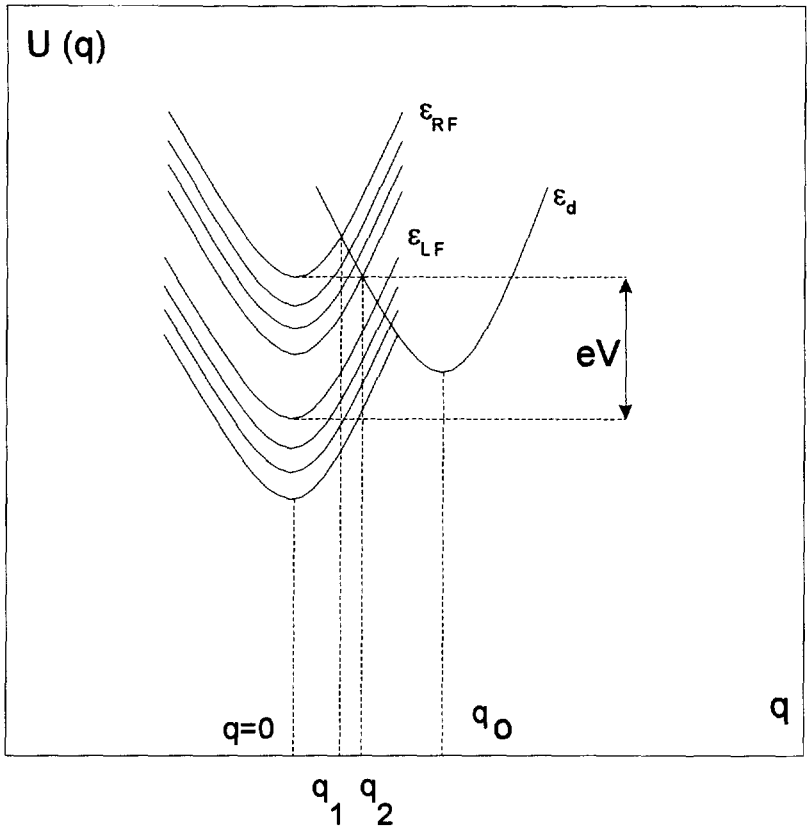

Fig. 6. Potential surface configurations corresponding to the STM patterns in Fig. 5. The three nuclear configurations q_0, q_1 and q_2 are shown.

5.2 Electronically resonating three-level STM transitions

The potential surfaces for ET between resonating substrate and tip levels, *via* the displaced adsorbate, coincide. As noted elsewhere [18, 99], this surface configuration is identical to the configuration in resonance Raman scattering or hot luminescence when a solute molecule is coupled *both* to a local high-frequency Raman active mode *and* to low-frequency conformational or solvent modes. The donor (say the substrate) and tip (acceptor) states correspond to the vibrational ground and first excited vibrational state of the Raman active mode while the *molecular* STM state corresponds to the (strongly displaced) electronically excited state in the optical scattering processes where the electronic and vibrational energy gaps are compensated by the energies of the incoming and scattered photon. With these observations close formal relations between the excitation profile or resonance Raman spectrum on the one side, and the bias potential or individual substrate or tip potential dependence of the STM current on the other, can be expected.

Closer analysis of these correlations will be provided elsewhere but we note presently the following. The differential cross section of a resonating photon from the frequency ν into a narrow frequency interval $\Delta\nu'$ centred at the frequency ν', and solid angle $\Delta\Omega$, is [108]

$$\Gamma = \frac{\Delta^2\sigma}{\Delta\nu'\Delta\Omega} = (3\pi)^{-1}\hbar^2(\nu'/c)^4 \times [(M_{eg}M_{ge})/(T_{eg}T_{ge})]^2 W_{th}^{(2)}(\Delta G_{eg}^0 - h\nu; h\nu' - h\nu) \quad (19)$$

where M_{eg}, M_{ge} are the transition dipoles, T_{eg}, T_{ge} the thermal electronic couplings between the ground and excited electronic states, and c the light velocity in the medium. $W_{th}^{(2)}$ is the three-level rate constant (s^{-1}) for the thermal analogue of the Raman scattering process and ΔG_{eg}^0 the Gibbs free energy gap between the ground and excited electronic states.

The STM resonance tunnel current is

$$i_{STM}^{res}(V/\eta) = (e/\hbar)\int d\epsilon_L \int d\epsilon_R\, d\, \rho_L(\epsilon_L)\rho_R(\epsilon_R) f(\epsilon_L) \times [1 - f(\epsilon_R)]\cdot W_{th}^{(2)}[\Delta G_{d-L}^0 + e\eta - (\epsilon_L - \epsilon_{LF}); eV \quad (20)$$

where the subscripts on ρ and ϵ refer to the positively and negatively biased electrode, respectively, η is the potential drop between the negatively biased electrode and the molecular centre, and $W_{th}^{(2)}$ has the same form as in Raman scattering. Equations (19) and (20)

therefore offer the following interesting implications for resonance STM:

(1) The potential drop $e\eta$ appears in the same form as the combination $\Delta G^0_{eg} - h\nu$. The $e\eta$-dependence therefore corresponds to the Raman *excitation profile* for a given transition. This would give a broad, peaked profile [108] with maximum where $|e\eta| \to E_r$. The peak is maintained in STM in spite of the continuous manifolds of levels since only a limited range of vacant levels, determined by the bias voltage, is available in the positively biased electrode. This is quite different from electrochemical ET where a much broader manifold can always participate and ensure current independence of η at large η. The STM maximum is thus broader the larger the bias potential. Such a maximum has recently been reported for *in situ* STM of a metalloporphyrin (*cf.* below) [109].

(2) The bias potential dependence can be recognized by noting that the resonance current dependence involving a given pair of levels in the left and right electrode follows that of the frequency combination $h\nu' - h\nu$ in the resonance Raman *spectrum*. Each microscopic level pair therefore contributes a narrow resonance. The overall current is the sum of the resonances over the bias potential range. The bias potential dependence is therefore weaker than the overpotential dependence. A stronger dependence can be expected if the potential variation distorts the tunnel barrier, or is reflected in the molecular level variation, causing this level to cross the Fermi level of the negatively biased electrode in certain bias potential ranges.

5.3 Off-resonance, vibrationally coherent or incoherent two-step STM transitions

These limits are representative of weak or intermediate coupling between the molecular level and both the substrate and tip. The full steady-state current forms for ET through the populated, vibrationally partially relaxed intermediate state is available elsewhere [100, 101]. The following simpler form is, however, obtained over quite broad electrode potential ranges

$$i^{STM}_{pop} \approx \frac{i^{equil}_{R-d}(\eta, V)[i^{equil}_{d-L}(\eta, V) + \pi\rho_L(\epsilon_L)i^{coh}_{d-L}(\eta, V)]}{i^{equil}_{R-d}(\eta, V) + i^{equil}_{d-L}(\eta, V)) + i^{coh}_{d-L}(\eta, V)}. \quad (21)$$

The superscript "equil" refers to the channel through the fully relaxed intermediate state. These terms are given by equations (5), (6), (10) and (13). "coh" refers to coherent ET through a vibrationally unrelaxed intermediate state. i^{coh}_{d-L} is represented approximately by the same equations except that the activation energy vanishes. In general, therefore the two channels may contribute comparably also when the electronic coupling is weak. If the electronic coupling in the second ET step is weak enough then the second term in equation (21) vanishes, and

$$i^{STM}_{pop} \approx \frac{i^{equil}_{R-d}(\eta, V)i^{equil}_{d-L}(\eta, V)}{i^{equil}_{R-d}(\eta, V) + i^{equil}_{d-L}(\eta, V)}. \quad (22)$$

This corresponds to two consecutive, fully equilibrated ET steps and is the STM mode in the strongly diabatic limit. Equations (21) and (22) hold the following further implications:

(1) As for resonating STM, coherent two-step STM is limited to the electronic levels in the positively biased electrode between the two Fermi levels. The overvoltage and bias potential dependence therefore follow patterns rather similar to those for resonance tunnelling even though the two processes are physically different. The data in [109] would thus be in line with both views and distinction must rest on other observations such as detection of the intermediate, vibrationally unrelaxed state.

(2) Equation (21) and coherent two-step ET apply when the electronic interaction between the molecular level and the positively biased electrode is strong enough that the second ET step proceeds prior to full intermediate state relaxation. The second step is then unlikely to succeed prior to relaxation and renewed activation, represented by equation (22) is needed. One of the two individual current terms would, furthermore, dominate over broad potential ranges. If the first step is the slower then the overvoltage dependence follows the pattern for electrochemical ET and reaches a plateau in the activationless overpotential range while the bias potential dependence is weak. If the second step is the slower then the first step is equilibrated and both the overpotential and bias potential dependence are strong, *ie* exponential. Characteristic overpotential and bias potential patterns for the different STM mechanisms thus provide a basis for mechanistic mapping.

(3) As for electrochemical ET the STM current can be extended in straightforward fashions to incorporate high-frequency quantum modes (*cf.* [101]). Vibrational "fine-structure" can thus be expected for the resonance and coherent two-step ET modes when the conditions $\hbar\Omega \geqslant \sqrt{E_r k_B T}$ and $\hbar\Omega \geqslant eV$ apply where E_r is the reorganization Gibbs free energy for the resonance tunnel process or the first coherent ET step, respectively.

(4) Equations (21) and (22) can be combined into a "unified" formalism if vibrational relaxation in the intermediate state is incorporated explicitly. Different approaches to this important aspect in the context of three-level processes have been discussed recently [25, 110].

6. CONCLUDING REMARKS

The electronic tunnel factor in long-range *homogeneous* chemical and biological ET has been characterized experimentally and theoretically in impressive detail. Outstanding questions are, however, associated with electronic interference among

different tunnel routes and environmentally induced tunnel barrier fluctuations. New and well characterized long-range *electrochemical* ET systems and the feasibility of STM mapping of large adsorbates also warrant new attention to the tunnel factor in interfacial ET between metallic electrodes and solvated molecules. Simple results can be obtained by density functional theory and overpotential dependent surface electronic density profiles. These can be converted self-consistently to the corresponding wave functions in more rigorous approaches. Work along these lines is in progress. A particular expectation is that surface charge variation can affect significantly the tunnel factor in long-range interfacial ET at surfaces of light metals, leading to observable asymmetric current–voltage relations with respect to the potential of zero charge.

The observation of facile long-range ET in homogeneous systems finally suggests that *in situ* STM of large adsorbate molecules which hold local, energetically accessible electronic levels such as in large transition metal complexes or redox metalloproteins, offers a new approach to interfacial ET mapping. The metal centres at the same time strongly facilitate tunnelling over long distances and lead to a variety of characteristic patterns for independent overpotential and bias potential control. This has been supported by the recent observation of *in situ* STM molecular patterns for cyt *c* [73] and of peak structure in the *in situ* STM current–voltage relation of metalloporphyrins.

ACKNOWLEDGEMENTS

We acknowledge financial support from the Danish Natural and Technical Science Research Councils, Volkswagen Stiftung, The European Research Programme INTAS, and the Russian Foundation for Fundamental Research.

REFERENCES

1. H. Sigel and A. Sigel, eds., *Metal Ions in Biological Systems*, **27,** M. Dekker, New York (1991).
2. H. B. Gray and J. R. Winkler, *Chem. Rev.* **92,** 369 (1992).
3. Contributions in: *Chem. Phys.* **176,** 289–649 (1993). Special Issue on Electron Transfer.
4. Contributions in: *J. Photochem. Photobiol. A: Chemistry* **92,** 1–236 (1994). Special Issue on Electron Transfer.
5. Contributions in: *Struct. Bond.* **75** (1991).
6. J. R. Miller, J. V. Beitz and R. K. Huddleston, *J. Am. Chem. Soc.* **106,** 5057 (1984).
7. G. Wiederrecht, S. Watanabe and M. R. Wasiliewski, *Chem. Phys.* **176,** 601 (1993).
8. C. C. Moser, J. M. Keske, K. Warncke, R. S. Farid and P. L. Dutton, *Nature* **355,** 796 (1992).
9. A. Ogrodnik, A. Keupp, M. Volk, G. Aumeier and M. E. Michel-Beyerle, *J. Phys. Chem.* **98,** 3422 (1994), and references therein.
10. T. Arlt, S. Schmidt, W. Kaiser, C. Lauterwasser, M. Meyer, H. Scheer and W. Zinth, *Proc. Nat. Acad. Sci. USA* **90,** 11757 (1993).
11. G. M. Ullmann and N. M. Kostic, *J. Am. Chem. Soc.* **117,** 4766 (1995).
12. G. Tollin, J. K. Hurley, J. T. Hazzard and T. E. Meyer, *Biophys. Chem.* **48,** 259 (1993).
13. A. G. Sykes, *Struct. Bond.* **75,** 175 (1991).
14. J. Deisenhofer and J. R. Norris, Eds., *The Photosynthetic Reaction Center*, Academic Press, New York, Vol. 2.
15. B. A. Heller, D. Holten and C. Kirmaier, *Science* **269,** 940 (1995), and references therein.
16. H. E. M. Christensen, L. S. Conrad, K. V. Mikkelsen, M. K. Nielsen and J. Ulstrup, *Inorg. Chem.* **29,** 2808 (1990).
17. G. McLendon, *Chem. Rev.* **92,** 481 (1992).
18. M. N. Paddon-Row, *Acc. Chem. Res.* **27,** 18 (1994), and references therein.
19. J. R. Reimers and N. S. Hush, *Chem. Phys.* **146,** 89 (1990), and references therein.
20. D. N. Beratan, J. N. Onuchic and J. J. Hopfield, *J. Chem. Phys.* **86,** 4488 (1987).
21. M. D. Newton, *Chem. Rev.* **91,** 767 (1991).
22. P. Siddarth and R. A. Marcus, *J. Phys. Chem.* **94,** 2985 (1990).
23. A. A. Stuchebrukhov and R. A. Marcus, *J. Phys. Chem.* **99,** 7581 (1995).
24. A. M. Kuznetsov and J. Ulstrup, *Phys. Status. Solidi. (b)* **114,** 673 (1982).
25. Yu. I. Kharkats, A. M. Kuznetsov and J. Ulstrup, *J. Phys. Chem.* **99,** 13545 (1995).
26. A. A. Kornyshev, A. M. Kuznetsov, U. Stimming and J. Ulstrup, *J. Phys. Chem.* **100,** 11175 (1996).
27. L. A. Khanova and M. R. Tarasevich, *J. Electroanal. Chem.* **227,** 115 (1987).
28. H. O. Finklea and D. D. Handshuh, *J. Am. Chem. Soc.* **114,** 3173 (1992).
29. A. M. Becka and C. J. Miller, *J. Phys. Chem.* **96,** 2657 (1992).
30. S. M. Becka and C. J. Miller, *J. Phys. Chem.* **97,** 6233 (1993).
31. H. O. Finklea, D. A. Snider, J. Fedyk, E. Sabatini, Y. Gafai and I. Rubinstein, *Langmuir* **9,** 3660 (1993).
32. S. Song, R. A. Clark, E. F. Bowden and M. J Tarlov, *J. Phys. Chem.* **97,** 6564 (1993).
33. C. E. D. Chidsey, *Science* **251,** 919 (1990).
34. J. F. Smalley, S. W. Feldberg, C. E. D. Chidsey, M. R. Lindford and M. D. Newton, *J. Phys. Chem.*, **99,** 13141 (1995).
35. V. G. Levich and R. R. Dogonadze, *Dokl. Akad. Nauk SSSR, Ser. Fiz. Khim.* **124,** 123 (1959).
36. V. G. Levich and R. R. Dogonadze, *Coll. Czech. Chem. Comm.* **26,** 193 (1961).
37. R. A. Marcus, *Ann. Rev. Phys. Chem.* **15,** 155 (1964).
38. N. R. Kestner, J. Logan and J. Jortner, *J. Phys. Chem.* **78,** 2148 (1974).
39. R. A. Marcus and N. Sutin, *Biochim. Biophys. Acta* **811,** 265 (1965).
40. A. M. Kuznetsov, J. Ulstrup and M. A. Vorotyntsev, in *The Chemical Physics of Solvation, Part C. Solvation in Specific Physical, Chemical and Biological Systems. p.* 163 (Edited by R. R. Dogonadze, E. Kálman, A. A. Kornyshev and J. Ulstrup) Elsevier, Amsterdam (1988).
41. A. M. Kuznetsov, *Charge Transfer in Physics, Chemistry and Biology*. Gordon and Breach, London (1995).
42. J. Ulstrup, *Charge Transfer Processes in Condensed Media*. Springer-Verlag, Berlin (1979).
43. H. M. McConnell, *J. Chem. Phys.* **35,** 508 (1961).
44. M. V. Vol'kenshtein, R. R. Dogonadze, A. K. Madumarov and Yu. I. Kharkats, *Dokl. Akad, Nauk SSSR, Ser. Fiz. Khim.* **199,** 124 (1971).
45. A. M. Kuznetsov and J. Ulstrup, *J. Chem. Phys.* **75,** 2047 (1981).

46. J. Jortner and M. Bixon, in *Protein Structure, Molecular and Electronic Reactivity* (Edited by R. Austin, E. Bukhs, B. Chance, D. DeVault, P. L. Dutton, H. Frauenfelder and V. I. Gol'danskij). p. 277. Springer-Verlag, New York (1987).
47. A. M. Kuznetsov, J. Ulstrup and M. D. Vigdorovich, *Chem. Phys.* **176,** 539 (1993).
48. J. P. Badiali, M. L. Rosinberg, F. Vericat and L. Blum, *J. Electroanal. Chem.* **158,** 253 (1983).
49. A. A. Kornyshev and M. A. Vorotyntsev, *J. Electroanal. Chem.* **167,** 1 (1984).
50. J.-P. Badiali, M.-L. Rosinberg and J. Goodisman, *J. Electroanal. Chem.* **143,** 73 (1983).
51. W. Schmickler and D. Henderson, *Progr. Surf. Sci.* **22,** 323 (1986).
52. W. Schmickler and D. Henderson, *J. Electroanal. Chem.* **290,** 283 (1990).
53. A. Mosyak, A. Nitzan and R. Kosloff, *J. Chem. Phys.*, **104,** 1549 (1996).
54. J. W. Schultze and K. J. Vetter, *Electrochim. Acta* **18,** 889 (1973).
55. J. W. Schultze and U. Stimming, *Z. Phys. Chem.* **98,** 285 (1975).
56. W. Schmickler and J. Ulstrup, *Chem. Phys.* **19,** 217 (1977).
57. W. Schmickler and J. W. Schultze, *Mod. Asp. Electrochemistry* **17,** 357 (1986).
58. R. R. Dogonadze, A. M. Kuznetsov and J. Ulstrup, *Electrochim. Acta* **22,** 967 (1977).
59. W. Schmickler, *J. Electroanal. Chem.* **113,** 159 (1980).
60. K. Doblhofer and J. Ulstrup, *J. Physique* **38,** C-49 (1977).
61. E. F. Dalton, N. A. Surridge, J. C. Jernigan, K. O. Wilbourn, J. S. Facci and R. W. Murray, *Chem. Phys.* **141,** 143 (1990).
62. D. A. Buttry and F. C. Anson, *J. Am. Chem. Soc.* **105,** 685 (1983).
63. J. Ulstrup, *Surf. Sci.* **101,** 564 (1980).
64. G. Intzelt, *Electronanal. Chem.* **15,** 89 (1991).
65. G. Huo and H. A. O. Hill, *Adv. Inorg. Chem.* **36,** 341 (1991).
66. A. Sucheta, R. Cammack, J. Weiner and F. A. Armstrong, *Biochemistry* **32,** 5455 (1993).
67. A. M. Bond, *Anal. Proc.* **29,** 132 (1992).
68. R. Guckenberger, W. Wiegräbe, A. Hillebrand, T. Hartmann, B. Wang and W. Baumeister, *Ultramicroscopy* **31,** 327 (1989).
69. R. Wiesenberger and M. J. Güntherodt (Eds.), *Scanning Tunnel Microscopy*. Springer-Verlag, Berlin (1992).
70. O. Marki and M. Arnrein (Eds.), *STM and AFM in Biology*. Academic Press, San Diego (1993).
71. L. Haggerty and A. M. Lenhoff, *Biotechnol. Progr.* **9,** 1 (1993).
72. G. J. Leggett, C. J. Roberts, P. M. Williams, M. C. Davies, D. E. Jackson and S. J. B. Tendler, *Langmuir* **9,** 2356 (1993).
73. J. E. T. Andersen, P. Møller, M. V. Pedersen and J. Ulstrup, *Surf. Sci.* **325,** 193 (1995).
74. Y. Degani and A. Heller, *J. Phys. Chem.* **91,** 1285 (1987).
75. H. Killesreiter and H. Baessler, *Chem. Phys. Lett.* **11,** 411 (1971).
76. M. Sugi, K. Nembach, D. Möbius and H. Kuhn, *Solid State Commun.* **15,** 1867 (1974).
77. H. Kuhn, *J. Photochem.* **10,** 111 (1979).
78. R. R. Dogonadze, in *Reactions of Molecules at Electrodes* (Edited by N. S. Hush) p. 135. Wiley, New York (1971).
79. R. R. Dogonadze and A. M. Kuznetsov, *Progr. Surf. Sci.* **6,** 1 (1975).
80. R. R. Dogonadze and A. M. Kuznetsov, in *Comprehensive Treatise of Electrochemistry, Vol.* 7. (Edited by J. O'M. Bockris, B. E. Conway and E. Yeager). p. 1. Plenum, New York (1979).
81. A. A. Kornyshev, A. M. Kuznetsov and J. Ulstrup, *J. Phys. Chem.* **98,** 3832 (1994).
82. P. G. Dzhavakhidze, A. A. Kornyshev and G. J. Tsitsuashvili, *Solid State Commun.* **52,** 401 (1984).
83. A. A. Kornyshev, in *The Chemical Physics of Solvation. Part C. Solvation in Specific Physical, Chemical and Biological Systems* (Edited by R. R. Dogonadze, E. Kálman, A. A. Kornyshev and J. Ulstrup) p. 355. Elsevier, Amsterdam (1988).
84. A. A. Kornyshev and A. M. Kuznetsov, *J. Mol. Liquids* **61,** 103 (1994).
85. W. Kohn and L. J. Sham, *Phys. Rev.* **140,** A1133 (1965).
86. J. Lipkowski, *Mod. Asp. Electrochemistry* **23,** 1 (1992).
87. A. A. Kornyshev, A. M. Kuznetsov, U. Stimming and J. Ulstrup, *J. Phys. Chem.* **100,** 11184 (1996).
88. O. G. Mouritsen and K. Jørgensen, *BioEssays* **14,** 129 (1992).
89. S.-K. Ma, *Modern Theory of Critical Phenomena*. Addison-Wesley, New York (1976).
90. A. Badia, R. Back and R. B. Lennox, *Angew. Chem.* **106,** 2429 (1994).
91. D. K. Luttrull, J. Graham, J. A. DeRose, D. Gust, T. A. Moore and S. M. Lindsay, *Langmuir* **8,** 765 (1992).
92. M. Kunitake, N. Batina and K. Itaya, *Langmuir* **11,** 2337 (1995).
93. M. Sumetskij, *J. Phys.: Condensed Matter* **3,** 2651 (1991).
94. M. Sumetskij and A. A. Kornyshev, *Phys. Rev.* **B48,** 17493 (1993).
95. M. Sumetskij, A. A. Kornyshev and U. Stimming, *Surf. Sci.* **307,** 23 (1993).
96. M. L. Lozano and M. C. Tringides, *Europhys. Lett.* **30,** 537 (1995).
97. D. M. Kolb, in Proceedings of the 46th ISE Meeting, Xiamen, p. K-1-2 (1995).
98. L. I. Glazman and R. I. Shekhter, *Sov. Phys. JETP* **94,** 282 (1987).
99. A. M. Kuznetsov and J. Ulstrup, *Chem. Phys.* **157,** 25 (1991).
100. A. M. Kuznetsov, P. Sommer-Larsen and J. Ulstrup, *Surf. Sci.* **275,** 52 (1992).
101. A. M. Kuznetsov and J. Ulstrup, *Surf. Coat. Tech.* **67,** 193 (1994).
102. W. Schmickler and C. Widrig, *J. Electroanal. Chem.* **336,** 213 (1992).
103. W. Schmickler, *Surf. Sci.* **295,** 43 (1993).
104. A. Müller, E. Diemann, K. Knüttel, A. Branting and K. Schneider, *Naturwiss.* **78,** 507 (1991).
105. P. Conolly, J. Cooper, G. R. Moore, J. Shen and G. Thompson, *Nanotechnol.* **2,** 160 (1991).
106. Z. Nawaz, T. R. I. Cataldi, J. Knall, R. Somekh and J. B. Pethica, *Surf. Sci.* **265,** 139 (1992).
107. J. E. T. Andersen, M. H. Jensen, P. Møller and J. Ulstrup, *Electrochim. Acta*, **41,** 2005 (1996).
108. M. G. Zakaraya and J. Ulstrup, *Chem. Phys.* **135,** 49 (1989).
109. N. J. Tao, *Phys. Rev. Lett.*, **76,** 4066 (1996).
110. H. Sumi and T. Kakitani, *Chem. Phys. Lett.* **252,** 85 (1996).